Migrating fibroblasts perform polarized, microtubule-dependent exocytosis towards the leading edge

Jan Schmoranzer[1,2], Geri Kreitzer[3] and Sanford M. Simon[1,*]

[1]Laboratory of Cellular Biophysics, The Rockefeller University, 1230 York Avenue, New York, NY 10021, USA
[2]Department of Biology, Chemistry, Pharmacology, Free University Berlin, 14195 Berlin, Germany
[3]Department of Cell and Developmental Biology, Weill Medical College of Cornell University, New York, NY 10021, USA
*Author for correspondence (e-mail: simon@mail.rockefeller.edu)

Summary

Cell migration might involve biased membrane traffic toward the leading edge to facilitate the building of extracellular matrix, membrane protrusions and adhesion plaques. We tested the hypothesis that secretory vesicles are preferentially delivered toward the leading lamella in wound-edge fibroblasts. Single fusion events of vesicles containing LDLR-GFP were mapped by total internal reflection fluorescence microscopy (TIR-FM). In migrating fibroblasts, exocytic events were polarized towards the leading edge. After disrupting microtubules with nocodazole, exocytosis continued, but fusion sites were clustered around central Golgi elements; there was no peripheral exocytosis. We conclude that microtubules are necessary for the domain-specific fusion of post-Golgi vesicles with the plasma membrane during migration.

Movies and supplemental data available online

Key words: Total internal reflection, Evanescent wave, Cell polarization, Post-Golgi vesicle, Migration, Secretion

Introduction

Fibroblasts develop pronounced morphological asymmetries when undergoing directed migration. This includes a large lamellipodium at the front and the nucleus at the back of the cell. The development of this asymmetry depends on cytoskeletal rearrangements and it has been proposed that polarization of membrane trafficking is also important in supporting migration. It was the goal of this work to test whether membrane traffic is polarized in migrating cells and whether the cytoskeleton contributes to this polarization.

Secretory cargo exits the Golgi in pleiomorphic membrane-bounded vesicles. Numerous live-cell studies have implicated microtubules in the transport of secretory cargo from the Golgi to the plasma membrane in mammalian fibroblasts (Lippincott-Schwartz et al., 2000). Upon depolymerization of microtubules with nocodazole, exocytic vesicles ceased to move and secretion of human chromogranin B was slowed (Wacker et al., 1997). In another study, the saltatory motion of post-Golgi vesicles carrying vesicular stomatitis virus glycoprotein-green fluorescent protein (VSVG-GFP) stopped after nocodazole treatment but the rate of bulk delivery to the plasma membrane was unchanged (Hirschberg et al., 1998). Similar to the findings in fibroblasts, some post-Golgi vesicles loaded with VSVG-GFP co-localized with microtubules in the cytosol of PtK$_2$ epithelial cells (Toomre et al., 1999). It is important to realize, however, that treatment of cells with microtubule antagonists also results in fragmentation and dispersal of the Golgi apparatus to peripheral regions of the cytoplasm (Cole et al., 1996). It is possible that redistribution of Golgi elements could bypass microtubule-mediated secretory traffic. Inhibition of microtubule-based transport with microinjected, function-blocking kinesin antibody leaves the Golgi intact but

completely abrogates transport of post-Golgi carriers containing neurotropin receptor (p75)-GFP towards the periphery of the cell in MDCK epithelial cells (Kreitzer et al., 2000).

In polarized epithelial cells, disruption of the microtubules slows the delivery of apical membrane proteins and often results in their mistargeting to the basolateral surface. By contrast, microtubule disruption does not significantly affect the delivery of basolateral membrane proteins but does induce apical exocytosis of proteins normally secreted into the basolateral medium (Boll et al., 1991; Thyberg and Moskalewski, 1999). Although the effects of microtubule disruption on apical and basolateral protein targeting in epithelia have been well characterized, it is unclear whether and how microtubules exert control over targeted transport of secretory carriers for fusion with specific domains of the plasma membrane. This is an important issue in highly polarized cells such as neurons and epithelia, in which the fidelity of asymmetric protein trafficking is essential to the function of these cells in situ. It is equally crucial in cells that transiently polarize in response to acute stimuli, such as fibroblasts migrating to close a wound.

Migration might require polarized exocytosis at the leading edge for the localized delivery of newly synthesized proteins and/or lipids, which are needed for adhesion and localized addition of membrane. For example, integrins are recycled to the front of migrating neutrophils via a Ca^{2+}-dependent mechanism (Lawson and Maxfield, 1995). Alternatively, local delivery of bulk membrane to the leading edge might help to form cell protrusions and could even drive migration (Bretscher, 1996). A third potential explanation for enhanced membrane traffic near the leading edge might be the modulation of

membrane tension to facilitate cellular protrusions during actin polymerization (Raucher and Sheetz, 2000).

To date, there has been no direct experimental evidence showing that mammalian fibroblasts perform polarized exocytosis towards the leading edge during migration. Early experiments on fixed cells showed a biased distribution of secretory cargo (VSV-G) towards the leading lamellae of wound-edge fibroblasts (Bergmann et al., 1983). However, because these studies were done using fixed cell assays, it is impossible to distinguish whether biased distribution was due to polarized secretion or to polarized retention of proteins in discrete membrane domains.

Total-internal-reflection fluorescence microscopy [TIR-FM (Axelrod, 1989)] has been used to image the final step of the secretory pathway – fusion of single vesicles with the plasma membrane (Steyer et al., 1997; Oheim et al., 1998; Schmoranzer et al., 2000; Toomre et al., 2000). Recently, we established a quantitative method for imaging single fusion events at the plasma membrane using TIR-FM (Schmoranzer et al., 2000). This method enabled us to distinguish fusion events from other vesicle behaviours such as movement out of the focal plane or photolysis. By locating individual fusion events in live cells, we can now investigate the spatial distribution of fusion sites at the plasma membrane and whether there are any preferred domains of exocytosis in mammalian cells. Specifically, we can test the hypothesis that exocytosis occurs preferentially at the leading edge of migrating fibroblasts. Furthermore, if domain-specific delivery of secretory cargo does occur in migrating fibroblasts, we can also test which cytoskeletal elements are involved in this process. Because microtubules support the long-range transport of post-Golgi carriers, we tested the role of the microtubule cytoskeleton in the site-specific delivery of secretory vesicles.

Here, we mapped the spatial distribution of fusion sites in migrating and stationary fibroblasts using time-lapse TIR-FM. Exocytosis of secretory vesicles was polarized towards the leading edge of migrating fibroblasts. After treatment with nocodazole to disrupt microtubules, transport and delivery of post-Golgi vesicles were abolished to the periphery of the cell in non-motile cells and to the leading edge of migrating, wound-edge cells.

Materials and Methods
Cell culture
Normal Rat Kidney (NRK) fibroblast were maintained in DMEM (Mediatech Cellgro, Herndon, VA) supplemented with 10% bovine calf serum, respectively, in a 37°C incubator humidified with 5% CO_2. Cells were plated either onto glass bottom dishes (MatTek, Ashland, MA) or on autoclaved coverslips (Fisher Scientific). For microscopy on stationary NRK fibroblasts, cells were plated at a high enough density such that they reached confluence within 1-2 days. Only cells that were in contact with the neighbouring cells were chosen for microscopy. For experiments on migrating fibroblasts, a densely confluent monolayer was wounded by scraping of rows of cells with a sterile pipette tip. Cells at the edge of the wound were allowed to recover for 2-3 hours at 37°C. Only cells with clearly polarized morphology, large lamellipodium and a nucleus away from the edge were chosen for microinjection.

Nuclear microinjection
Cells were microinjected with constant pressure into the nucleus with cDNAs encoding the green fluorescent protein (GFP) chimera of a recycling-deficient mutant of the low-density-lipoprotein receptor (LDLRa18, 15 μg ml^{-1}). The cDNA was prepared in HKCl microinjection buffer (10 mM HEPES, 140 mM KCl, pH 7.4) and microinjected using back-loaded glass capillaries and a micromanipulator (Narishige, Greenvale, NY). After injection, the cells were maintained at 37°C in a humidified CO_2 environment for 60 minutes to allow the expression of injected cDNAs. Newly synthesized protein was accumulated in the Golgi/trans-Golgi network by incubating cells at 20°C (1-3 hours) in bicarbonate-free DMEM supplemented with 5% serum and 100 μg ml^{-1} cycloheximide (Sigma Chemicals, St Louis, MO). Cells were transferred to recording medium (Hanks Balanced Salt Solution, supplemented with 20 mM HEPES, 1% calf serum, 4.5 g l^{-1} glucose, 100 μg ml^{-1} cycloheximide). After shifting to the permissive temperature of 32°C for transport out of the Golgi, the arrival of vesicles labelled with LDLRa18-GFP was monitored by time-lapse TIR-FM. Nocodazole was obtained from Sigma (Sigma Chemicals, St Louis, MO).

Image acquisition
The illumination for TIR-FM was done through the objective as previously described (Schmoranzer et al., 2000). It consists of an inverted epifluorescence microscope (IX-70, Olympus America, Melville, NY) equipped with high-numerical-aperture lenses (Apo 100× NA 1.65, Apo 60× NA 1.45; Olympus) and a home-built temperature controlled enclosure. LDLR-GFP-tagged proteins were excited with the 488 nm line of an argon laser (Omnichrome, model 543-AP A01; Melles Griot, Carlsbad, CA) reflected off a dichroic mirror (498DCLP). All filters were obtained from Chroma Technologies (Brattleboro, VT).

Images were acquired with a 12-bit cooled CCD (either Orca I C4742-95 or ORCA-ER, Hamamatsu Photonics, Bridgewater, NJ) both with a resolution of 1280×1024 pixels [pixel sizes of (6.70 μm)^2 and (6.45 μm)^2, respectively]. The camera, the NI-IMAQ 1424 image acquisition card (National Instruments, Austin, TX) and a mechanical shutter (Uniblitz, Vincent Associates, Rochester, NY) were controlled by in-house software written in LABVIEW™ 6.1 using the IMAQ Vision package (National Instruments). Images were acquired with full spatial resolution at 4-5 frames per second. Images containing a region of interest of the cell were streamed to memory on a PC during acquisition and then saved to hard disk. The number of frames acquired per continuous sequence was limited by the size of the memory (~100-500 kB per image depending upon the size of the region of interest and the binning mode of the camera). The depth of the evanescent field was typically ~70-120 nm for the Apo 60× N.A. 1.45 lens (Schmoranzer et al., 2000).

Cells were chosen that had an even adherence to the coverslip. The initial 1 hour of expression after microinjection allowed sufficient time for some newly synthesized protein to reach the plasma membrane. Thus, we evaluated the adherence pattern based on the uniformity of LDLR-GFP at the plasma membrane.

Mapping of fusion sites
Processing and analysis of the video sequences was done either with in-house software written in LABVIEW 6.1 using the IMAQ Vision package or with MetaMorph (Universal Imaging, Downingtown, PA). The sites of fusion were mapped manually using in-house software written in LABVIEW 6.1. By systematically cropping the whole field of view into smaller, easily viewable areas, the video sequences were viewed repeatedly with different look-up tables to localize the fusion events. The times of docking and fusion start, and the coordinates of the fusion sites were catalogued. The coordinates were plotted in Origin® (OriginLab, Northampton, MA) and then overlayed with the epifluorescence image of the cell taken at the start of release of the Golgi block.

Results

Monitoring fusion during TIR-FM

To monitor exocytic fusions in live cells, we expressed the membrane protein LDLR-GFP via nuclear microinjection and accumulated newly synthesized protein in the Golgi/trans-Golgi network by incubating the cells at 20°C. After ~1 hour of accumulation, cells were shifted to 32°C, a temperature permissive for transport out of the Golgi. The distribution of newly expressed LDLR-GFP 10 minutes after release of the Golgi block was observed using either conventional epifluorescence microscopy or TIR-FM (Fig. 1). In epifluorescence (Fig. 1A), the whole cell is illuminated and LDLR-GFP was observed primarily in the juxtanuclear Golgi complex. By contrast, in TIR-FM images (Fig. 1B), only the region of the cell in contact with the substratum is illuminated by the evanescent field (~100 nm into the cell). Time-lapse TIR-FM recordings showed that individual vesicles could be seen moving along the plasma membrane until they stopped and fused (Fig. 1C,D, Movies A,C). Fusion of a vesicle is defined quantitatively by the simultaneous rise of total and width of the fluorescence intensity of the vesicle (Fig. 1E) (Schmoranzer et al., 2000). By TIR-FM, we observed vesicles fusing with the plasma membrane as early as 10 minutes after release of the Golgi block, and fusion continued for up to ~120 minutes until the LDLR-GFP was completely emptied from the Golgi.

Exocytosis is polarized towards the leading edge in migrating fibroblasts

We tested for domain-specific delivery of biosynthetic membrane cargo (LDLR-GFP) in fibroblasts by mapping the vesicle fusion sites in stationary and migrating NRK cells. Vesicle fusion was detected by TIR-FM as described above and the positions of fusion sites (from images acquired over a 60 minute period) were mapped (see Materials and Methods). Uneven adherence of cells might bias the TIR-FM fusion analysis, which relies on the plasma membrane being in close contact with the coverslip. Thus, in all experiments, we selected only cells that showed a uniform adherence pattern as detected by the fluorescence signal of the plasma membrane in TIR-FM at the beginning of the experiment.

In all mapping experiments (Fig. 2), the fusion sites were superimposed on the outline of the cell (yellow line) and an epifluorescence image showing the location of the cargo (LDLR-GFP) at the beginning of Golgi-block release. At this time most of the cargo was accumulated in the Golgi. In stationary cells (cells grown to confluence), the resulting map revealed that fusion events were widely distributed over the cell surface (Fig. 2A, Movie A), with areas of sparse and areas of more clustered fusion sites. In general, most vesicles were transported away from the Golgi towards the periphery of the cell until they fused.

To test whether the delivery of post-Golgi vesicles in
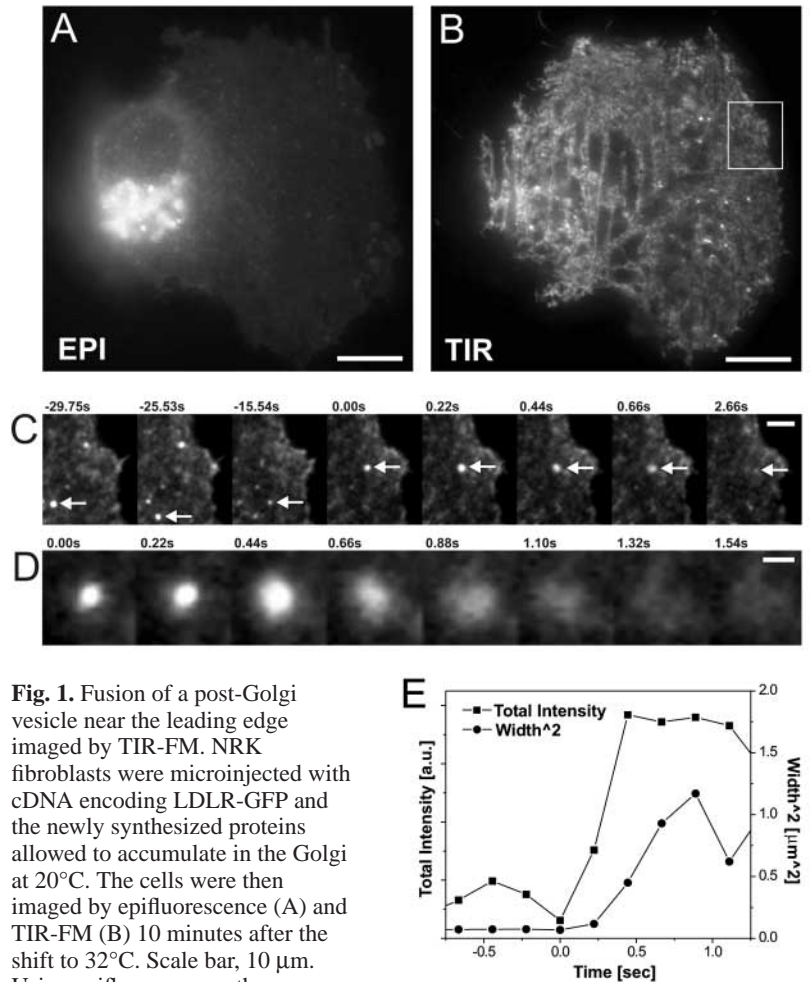
Fig. 1. Fusion of a post-Golgi vesicle near the leading edge imaged by TIR-FM. NRK fibroblasts were microinjected with cDNA encoding LDLR-GFP and the newly synthesized proteins allowed to accumulate in the Golgi at 20°C. The cells were then imaged by epifluorescence (A) and TIR-FM (B) 10 minutes after the shift to 32°C. Scale bar, 10 μm. Using epifluorescence, the accumulated LDLR-GFP brightens the area of the Golgi complex. Using TIR-FM on the same cell, single vesicles can be seen that have arrived at the contact surface. (C) An enlargement of a vesicle moving toward the leading edge and (D) fusing with the plasma membrane. Scale bars, 2 μm (C), 1 μm (D). (E) Plots of the total intensity and the width of the fluorescence intensity of the fusion event in (D). Time is indicated relative to moment of fusion start at 0.00 seconds.

migrating fibroblasts differs from that in stationary cells, we measured the frequency and distribution of fusion events in cells at the edge of an experimental wound. To ensure that the injected cells were migrating, we monitored the position of the cells before and after the TIR-FM recordings (Fig. 3). Similar to previous observations, only two-thirds of these cells had their Golgi oriented towards the front of the cell (Palazzo et al., 2001). For example, the Golgi complex of the cell shown in Fig. 3D is so oriented, whereas the Golgi of the cell in Fig. 2C is not. Thus, Golgi reorientation was not used as the criterion for migration.

The map of post-Golgi vesicle fusions in migrating cells differed dramatically from that in stationary cells. Strikingly, many fusion sites were clustered close to the leading edge of migrating cells (representative example of four migrating cells in Fig. 2D and Movies C front and back). This distribution of fusion sites was quantified in two ways. First, the distance between the fusion site and the Golgi was measured as a function of the maximum distance between the Golgi and the

Fig. 2. Map of fusion sites of post-Golgi vesicles. NRK fibroblasts were microinjected with cDNA encoding LDLR-GFP and imaged using TIR-FM with a temporal resolution of ~5 frames per second between 10 minutes and 60 minutes after the release of the Golgi block. Cells were outlined (yellow line) by thresholding the epifluorescence image against the background. Epifluorescence images indicate the LDLR-GFP load in the Golgi before the release of the Golgi block (grey level). The sites of fusion are indicated by either yellow crosses or cyan stars, depending on whether the fusions were complete or partial, respectively. For the migrating cells (C,D), the direction of the leading edge is indicated by white arrows. Stationary (A,B) and migrating (C,D) cells are either untreated (A,C) or treated with 10 µM nocodazole (B,D) during the last hour of the 3-hour Golgi block. Scale bars, 10 µm.
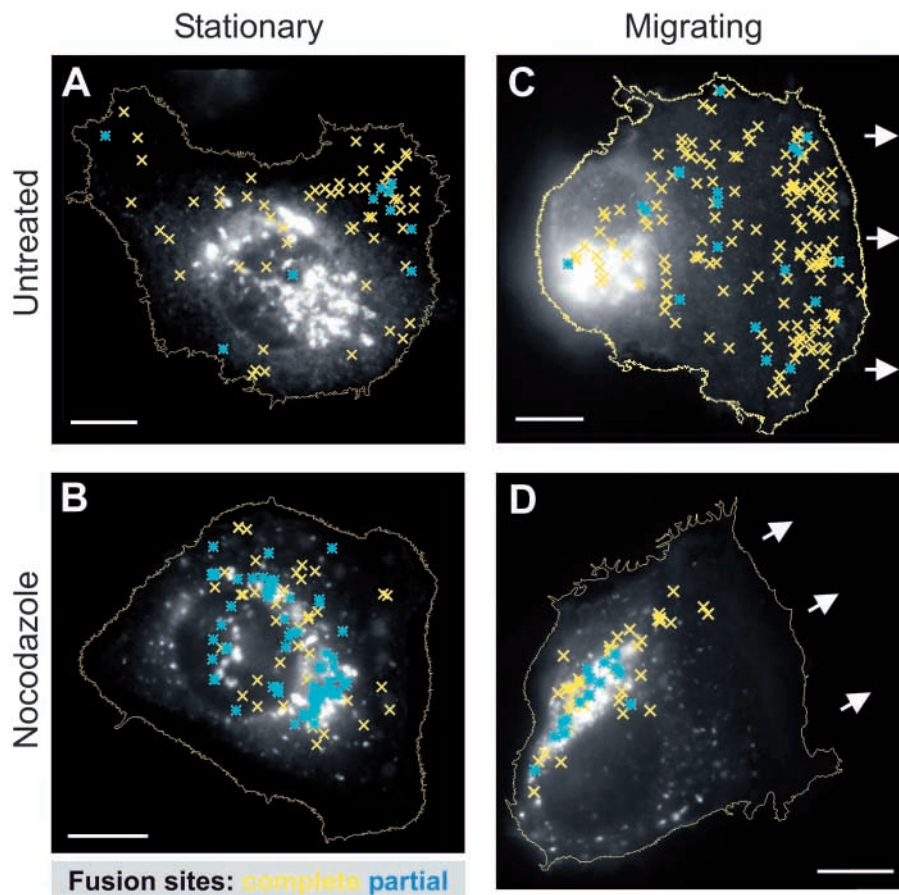
periphery of the cell (Fig. 4A,B). Because vesicles are transported along curvilinear microtubule tracks, this measurement does not record the true distance travelled. However, this analysis can be used to compare the statistical distributions of the values from cells under different conditions. In stationary cells, the distance values show an even distribution, falling off gradually at about 40% of the maximum distance between the Golgi centre and the farthest edge of the cell (Fig. 4A). The fusions were significantly farther from the Golgi in migrating, wound-edge cells (peak at ~65%, average at ~44%) than in stationary cells (peak at ~15%, average at ~21%) (Fig. 4A,B). Approximately half of all fusion sites were mapped at a position greater than
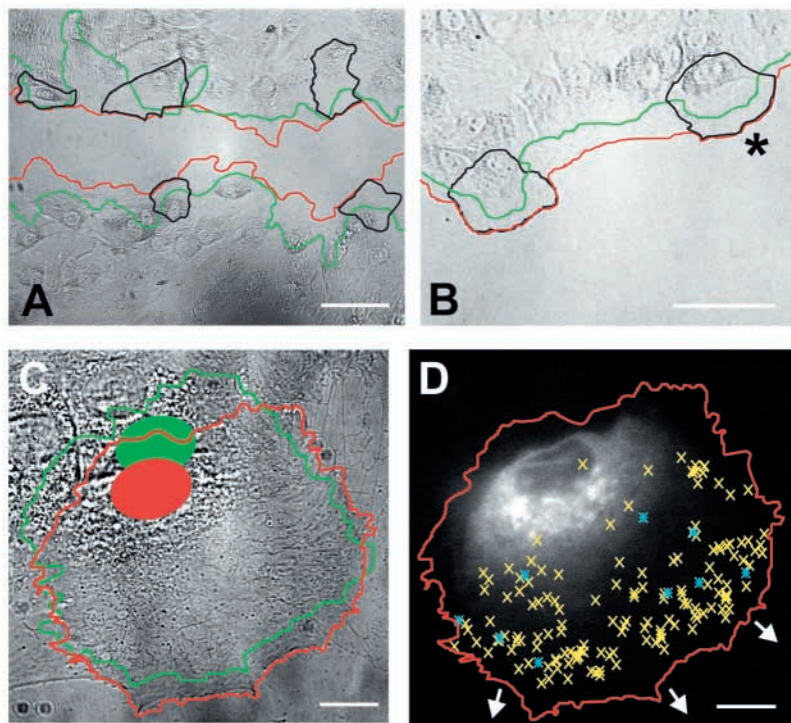
Fig. 3. Microinjected cells move during TIR-FM recording of exocytic events. (A,B) Monolayers of NRK fibroblasts were wounded. Cells at the edge of the wound were microinjected with cDNA encoding LDLR-GFP, incubated for 1 hour at 37°C and then shifted to 20°C for 2 hours prior to image acquisition. Wound-edge cells expressing LDLR-GFP were identified at low magnification by epifluorescence (black outlines). The cells were then imaged under transmitted light at the same magnification to localize the wound edge at the beginning of the experiment (green outline). At the end of the experiment, ~90 minutes later, the same field was imaged again at low magnification (red outline). Cells at the edge of the wound advanced significantly (10-20 µm) during that time. All injected cells advanced with the wound edge. (C) High magnification contrast images were taken of the injected cell marked by the asterisk in (B). The outlines of the cell and the nuclei were traced just before the first TIR-FM recording (0 min, green) and after the last TIR-FM recording (30 min, red). (D) The cell shown in (C) was imaged by TIR-FM in eight intervals (each 500 frames, 5 frames per second). The complete (yellow crosses) and partial (cyan stars) fusion events were mapped. The fusion map was overlayed on top of an epifluorescence image taken at the beginning of the TIR-FM recording. Notice that the Golgi complex is oriented towards the direction of migration (white arrows). Scale bars, 50 µm (A,B); 10 µm (C,D).
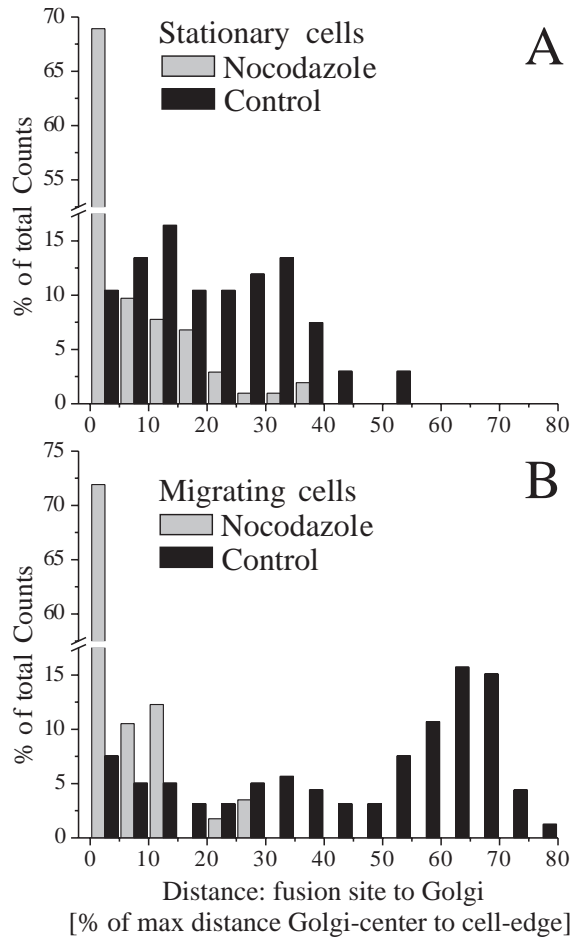
Fig. 4. Distances of fusion sites of vesicles from the nearest Golgi element in untreated or nocodazole-treated stationary and migrating fibroblasts. The distances from each site of fusion (mapped in Fig. 2) to the closest Golgi element (before the release of the Golgi block) were measured for stationary (A) and migrating (B) cells. The data from untreated and nocodazole-treated cells are coded in black and grey, respectively. To normalize for cell size, the distance values are displayed as the percentage of the maximal distance between the centre of the Golgi and the furthest edge of the cell. The counts are normalized to the total counts (notice the axis break).

Fig. 5. Distribution of the fusion density and time in stationary and migrating NRK fibroblasts. For each cell, the long axis was defined as the furthest distance from edge to edge through the centre. The total region of the cell was then divided into three orthogonal parts with equal width along the long axis (A). To compare migrating and stationary cells, we chose region 1 to be at the end of each cell that was closest to the nucleus. The number of fusion sites were counted in each region and normalized by the total number of fusions per cell. The fusion density was determined by dividing the normalized number of fusions per region by the normalized area of each region. To account for the higher fusion rate in migrating cells (~22 fusions per minute) compared with stationary cells (about eight fusions per minute), the values for the migrating cells were multiplied by 2.75. These fusion-density/time values of each cell [five stationary cells (176 fusions) and four migrating cells (375 fusions)] were averaged and plotted with the SEM as error bar (B).

50% of the distance between the Golgi and the cell periphery. This clearly demonstrates that post-Golgi vesicles are transported over a longer distance in migrating versus stationary cells.

Second, the polarization of fusion sites was quantified by measuring fusions per unit time in each of three equally spaced areas along the long axis of the cells (Fig. 5A,B). Compared with stationary cells (*n*=5), migrating cells (*n*=4) clearly showed strongly biased exocytosis within the region of the cell including the leading edge (region 3). The number of fusions occurring at the leading edge might be an underestimate because some regions of the lamellipodium might not be close enough to the coverslip to be detected by TIR-FM. Indeed, many vesicles moving towards the leading edge disappeared abruptly without undergoing obvious fusion. It is possible that these vesicles fused with regions of the plasma membrane outside the evanescent field (i.e. the ventral plasma membrane

domain). This would be consistent with our observation of a sharply bordered exclusion of fusion sites ~1-2 μm short of the cell edge. However, it is also possible that vesicular transport into this region is restricted by a dense actin meshwork at the leading edge.

Migrating cells exhibited a higher fusion rate (about 22 fusions per minute, 353 fusions in four cells) than stationary cells (about eight fusions per minute, 181 fusions in four cells). Near the trailing edge of migrating cells, the rate of fusions per unit area was comparable to the rate of fusions across the contact surface of stationary cells. By contrast, near the leading edge of migrating cells, the rate of fusions was significantly higher (Fig. 5).

We have previously observed that not all fusion events result in complete emptying of cargo from the secretory vesicles (Schmoranzer and Simon, 2003). When we analysed the number of partial and complete fusion events in stationary cells we found that, in 14% of all fusion events (*n*=181 in four

cells), only part of the membrane protein cargo of each vesicle was delivered to the plasma membrane. An example cell is shown in Fig. 2A in which vesicles that completely delivered their cargo are marked with yellow crosses and those that delivered only part of the membrane cargo are marked with cyan stars. The spatial distributions of complete- and partial-release fusions could not be distinguished. A similar population of partial-release fusion events was observed in the migrating cells (13% of 353 fusions in four cells; Fig. 2C, Fig. 3D).

Disruption of microtubules eliminates long-range, polarized delivery of post-Golgi vesicles to the cell periphery

To test the role of microtubules in the targeted delivery of post-Golgi vesicles, we treated the cells with 10 µM nocodazole during the last hour of the Golgi block. After this treatment, microtubules were largely, but not completely, depolymerized (see supplementary Fig. S1, http://jcs.biologists.org/supplemental/). Although the Golgi was fragmented slightly under these conditions, most of the Golgi elements were still located in a juxtanuclear position (Fig. 2B,D). Post-Golgi cargo appeared as large fluorescent spots that underwent little, if any, directional transport. Fusion events, however, were still observed, albeit at a reduced rate (about four fusions per minute, 185 fusions).

We repeated the mapping experiment in nocodazole-treated cells. At the wound edge, these cells exhibited the same polarized morphology as the non-treated wound-edge cells but, as expected, they did not migrate. Therefore, we called the nocodazole-treated wound-edge cells simply 'polarized' cells. In both stationary cells in a confluent monolayer (Fig. 2B) and polarized cells at the edge of a wound (Fig. 2D), the fusion sites were clustered around the partially dispersed Golgi elements. As a result, the distribution of fusion sites is dramatically shifted to smaller values, with ~70% of all fusion sites clustered between 0% and 5% (notice the break in the vertical axis in Fig. 4A,B). Very few fusions occurred at the cell periphery. This result clearly demonstrates that long-range vesicle transport toward the cell periphery is microtubule dependent. Significantly, the proportion of partial fusion events increased from 13% in untreated cells to 54% in nocodazole treated cells (Fig. 2B,D).

Discussion

Microtubules are involved in the long-range transport of organelles, including post-Golgi vesicles (Hirschberg et al., 1998; Toomre et al., 1999). However, because secretion continues in the presence of microtubule antagonists, the precise role of microtubules in secretion is unclear. It was suggested that microtubules might be responsible for delivering post-Golgi vesicles to specific regions within the plasma membrane.

Using TIR-FM, we previously established a quantitative method for imaging single fusion events of constitutively secreted vesicles at the plasma membrane (Schmoranzer et al., 2000). This method enabled us to locate single fusion events over a large area of a living cell. Using this technique, we observed that secretory vesicles remain attached to the

microtubules even as the vesicle is fusing and delivering membrane cargo to the plasma membrane (Schmoranzer and Simon, 2003).

Here, we show directly, by mapping the fusion sites of post-Golgi vesicles in live cells, that intact microtubules are responsible for the delivery of vesicles to certain domains on the cell surface. In untreated, stationary cells, fusion sites were widely distributed over the cell surface. In migrating cells the fusions were strongly polarized towards the leading edge.

With disruption of the microtubule array, fusion of post-Golgi vesicles still occurred. However, the fusion behaviour changed in two ways. (1) All fusion sites were clustered around the central Golgi elements. We can therefore conclude that long-range transport from the central Golgi to the plasma membrane is clearly dependent on microtubules. (2) In the absence of microtubules, a substantial proportion of vesicles require repeated fusions to deliver all of their membrane proteins to the plasma membrane. This is consistent with our previous observations that the microtubules affect the dynamics of vesicular fusion (Schmoranzer and Simon, 2003). Mapping the partial and complete releases, we see no bias of the partial fusions toward the leading lamellae in migrating cells.

It has been proposed that migration might require polarized exocytosis at the leading edge for delivery of recycled proteins such as integrins (Lawson and Maxfield, 1995), secretory proteins (Bergmann et al., 1983) or bulk membrane (Bretscher, 1996). However, like the enhanced exocytosis we observed at the leading edge, we recently found that endocytosis is enhanced near the leading edge (Rappoport and Simon, 2003). Thus, it does not seem likely that the net addition of bulk membrane by enhanced exocytosis at the leading edge is required to drive migration. The enhanced exocytosis and endocytosis could instead be a mechanism by which to promote rapid and reversible modifications in the protein and lipid composition, and/or the tension of the membrane at the leading edge. Enhanced exocytosis might contribute to the delivery of new membrane and secretory proteins toward the leading edge. Alternatively, a change in membrane tension might facilitate the formation of cellular protrusions during actin remodelling (Raucher and Sheetz, 2000). Either scenario, alone or in combination, could be forces that contribute to cell migration.

Our data show that microtubules are required for peripheral and domain-specific exocytosis in fibroblasts. Disruption of microtubules has been shown to stop or reduce locomotion of fibroblasts (Vasiliev et al., 1970; Gail and Boone, 1971; Goldman, 1971; Liao et al., 1995). Injection of an antibody against kinesin results in reduction of cell asymmetry and suppression of pseudopodial activity at the leading edge of migrating fibroblasts (Rodionov et al., 1993). Injection of an antibody against kinesin also blocks microtubule-based transport of secretory cargo from the Golgi to the cell periphery (Kreitzer et al., 2000). Together, these results support the hypothesis that polarized exocytosis is required for migration.

How localized secretion contributes to migration and the mechanism by which secretory carriers are directed to the leading lamella in migrating fibroblasts remain to be resolved. Clearly, this targeting is microtubule dependent but it is still unknown how vesicles end up on correct microtubule tracks for their destination.

Reference

Axelrod, D. (1989). Total internal reflection fluorescence microscopy. *Methods Cell Biol.* **30**, 245-270.

Bergmann, J. E., Kupfer, A. and Singer, S. J. (1983). Membrane insertion at the leading edge of motile fibroblasts. *Proc. Natl Acad. Sci. USA* **80**, 1367-1371.

Boll, W., Partin, J. S., Katz, A. I., Caplan, M. J. and Jamieson, J. D. (1991). Distinct pathways for basolateral targeting of membrane and secretory proteins in polarized epithelial cells. *Proc. Natl. Acad. Sci. USA* **88**, 8592-8596.

Bretscher, M. S. (1996). Moving membrane up to the front of migrating cells. *Cell* **85**, 465-467.

Cole, N. B., Sciaky, N., Marotta, A., Song, J. and Lippincott-Schwartz, J. (1996). Golgi dispersal during microtubule disruption: regeneration of Golgi stacks at peripheral endoplasmic reticulum exit sites. *Mol. Biol. Cell* **7**, 631-650.

Gail, M. H. and Boone, C. W. (1971). Effect of colcemid on fibroblast motility. *Exp. Cell Res.* **65**, 221-227.

Goldman, R. D. (1971). The role of three cytoplasmic fibers in BHK-21 cell motility. I. Microtubules and the effects of colchicine. *J. Cell Biol.* **51**, 752-762.

Hirschberg, K., Miller, C. M., Ellenberg, J., Presley, J. F., Siggia, E. D., Phair, R. D. and Lippincott-Schwartz, J. (1998). Kinetic analysis of secretory protein traffic and characterization of Golgi to plasma membrane transport intermediates in living cells. *J. Cell Biol.* **143**, 1485-1503.

Kreitzer, G., Marmorstein, A., Okamoto, P., Vallee, R. and Rodriguez-Boulan, E. (2000). Kinesin and dynamin are required for post-Golgi transport of a plasma-membrane protein. *Nat. Cell Biol.* **2**, 125-127.

Lawson, M. A. and Maxfield, F. R. (1995). Ca^{2+}- and calcineurin-dependent recycling of an integrin to the front of migrating neutrophils. *Nature* **377**, 75-79.

Liao, G., Nagasaki, T. and Gundersen, G. G. (1995). Low concentrations of nocodazole interfere with fibroblast locomotion without significantly affecting microtubule level: implications for the role of dynamic microtubules in cell locomotion. *J. Cell Sci.* **108**, 3473-3483.

Lippincott-Schwartz, J., Roberts, T. H. and Hirschberg, K. (2000). Secretory protein trafficking and organelle dynamics in living cells. *Annu. Rev. Cell Dev. Biol.* **16**, 557-589.

Oheim, M., Loerke, D., Stühmer, W. and Chow, R. H. (1998). The last few milliseconds in the life of a secretory granule – docking, dynamics and fusion visualized by total internal reflection fluorescence microscopy (TIRFM). *Eur. Biophys. J. Biophys. Lett.* **27**, 83-98.

Palazzo, A. F., Joseph, H. L., Chen, Y., Dujardin, D. L., Alberts, A. S., Pfister, K. K., Vallee, R. B. and Gundersen, G. G. (2001). Cdc42, dynein, and dynactin regulate MTOC reorientation independent of Rho-regulated microtubule stabilization. *Curr. Biol.* **11**, 1536-1541.

Rappoport, J. Z. and Simon, S. M. (2003). Real-time analysis of clathrin mediated endocytosis during cell migration. *J. Cell Sci.* **116**, 847-855.

Raucher, D. and Sheetz, M. P. (2000). Cell spreading and lamellipodial extension rate is regulated by membrane tension. *J. Cell Biol.* **148**, 127-136.

Rodionov, V. I., Gyoeva, F. K., Tanaka, E., Bershadsky, A. D., Vasiliev, J. M. and Gelfand, V. I. (1993). Microtubule-dependent control of cell shape and pseudopodial activity is inhibited by the antibody to kinesin motor domain. *J. Cell Biol.* **123**, 1811-1820.

Schmoranzer, J. and Simon, S. M. (2003). Role of microtubules in fusion of post-Golgi vesicles to the plasma membrane. *Mol. Biol. Cell* **14**, 1558-1569.

Schmoranzer, J., Goulian, M., Axelrod, D. and Simon, S. M. (2000). Imaging constitutive exocytosis with total internal reflection fluorescence microscopy. *J. Cell Biol.* **149**, 23-32.

Steyer, J. A., Horstmann, H. and Almers, W. (1997). Transport, docking and exocytosis of single secretory granules in live chromaffin cells. *Nature* **388**, 474-478.

Thyberg, J. and Moskalewski, S. (1999). Role of microtubules in the organization of the Golgi complex. *Exp. Cell Res.* **246**, 263-279.

Toomre, D., Keller, P., White, J., Olivo, J. C. and Simons, K. (1999). Dual-color visualization of trans-Golgi network to plasma membrane traffic along microtubules in living cells. *J. Cell Sci.* **112**, 21-33.

Toomre, D., Steyer, J. A., Keller, P., Almers, W. and Simons, K. (2000). Fusion of constitutive membrane traffic with the cell surface observed by evanescent wave microscopy. *J. Cell Biol.* **149**, 33-40.

Vasiliev, J. M., Gelfand, I. M., Domnina, L. V., Ivanova, O. Y., Komm, S. G. and Olshevskaja, L. V. (1970). Effect of colcemid on the locomotory behaviour of fibroblasts. *J. Embryol. Exp. Morphol.* **24**, 625-640.

Wacker, I., Kaether, C., Kromer, A., Migala, A., Almers, W. and Gerdes, H. H. (1997). Microtubule-dependent transport of secretory vesicles visualized in real time with a GFP-tagged secretory protein. *J. Cell Sci.* **110**, 1453-1463.